Optical Design of the Submillimeter Wave Instrument on JUICE

Mikko Kotiranta[1,*], Axel Murk[1], Karl Jacob[1], Hyunjoo Kim[1], and Paul Hartogh[2]
[1]Institute of Applied Physics, University of Bern, 3012 Bern, Switzerland
[2]Max Planck Institute for Solar System Research, 37077 Göttingen, Germany
*Contact: mikko.kotiranta@iap.unibe.ch

Abstract— **The upcoming Submillimeter Wave Instrument on the JUICE spacecraft is a passive dual-beam heterodyne radiometer operating in the frequency bands 530 – 625 GHz and 1080 – 1275 GHz. The instrument will observe Jupiter's atmosphere as well as the atmospheres and surface properties of its moons. This work presents the optical design and analysis of the instrument that has been carried out using Gaussian beam mode analysis and physical optics simulations. The optics consists of a mechanically steerable off-axis Cassegrain telescope, relay optics and two feedhorns. Frequency independent operation of the 600-GHz channel is predicted by the simulations. The 1200-GHz channel shows some frequency dependency because of the selected feedhorn type. The scanning of the telescope affects mainly its cross-polarization level.**

I. Introduction

The JUpiter ICy moons Explorer (JUICE) is an ESA large-class mission to Jupiter and its satellites. The launch is scheduled for 2022. The spacecraft carries 10 instruments on-board, one of them being the Submillimeter Wave Instrument (SWI), which is a passive dual-beam heterodyne radiometer for the frequency bands 530 – 625 GHz and 1080 – 1275 GHz [1]. The telescope and receiver unit (TRU) of the instrument is depicted in Fig. 1. Additionally, the instrument consists of an electronic unit with different high resolution and broadband spectrometers, and a radiator unit which provides passive cooling down to a temperature of 120 K for the Schottky diode mixers and low-noise amplifiers of the receiver unit.

The scientific objectives of SWI include the investigation of the temperature distribution, chemical composition and dynamics of Jupiter's stratosphere, as well its coupling to other atmospheric regions. The atmospheres, their interaction with the Jovian magnetosphere, and the surface properties of the icy moons Callisto, Europa, and Ganymede will be characterized as well. SWI will therefore provide information that is complementary to the data provided by the Microwave Radiometer (MWR) on the Juno spacecraft [2] that is currently performing observations of the lower parts of Jupiter's atmosphere in the frequency band 0.6 – 22 GHz.

The optics of the SWI has been first discussed in [3]. Notable design changes have since taken place, the most important of them being the inclusion of a 1200-GHz receiver channel. Other changes initiated by refined structural requirements include adjustments of the optical element sizes and positions. This paper presents the current optical design and analysis that is based on Gaussian beam mode analysis [4] and physical optics (PO) [5] simulations.

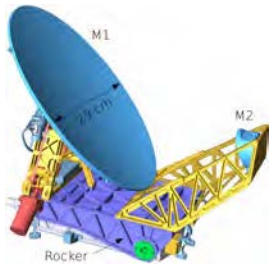

Fig. 1. CAD-model of the Submillimeter Wave Instrument.

II. Optical Design

SWI receives the signal of interest with an off-axis Cassegrain telescope. Its paraboloidal main mirror (M1) has a projected diameter of 29 cm while the hyperboloidal secondary mirror (M2) has a projected diameter of 6 cm. The telescope is mounted on a rocker that can be tilted ±4.3° to allow scanning perpendicular to the spacecraft orbital plane (cross-track). Scanning in the orbital plane (along-track) is possible by rotating the mirror M1 up to ±72°. The scanning mechanisms enable observations along Jupiter's limb, mapping of the icy moons with variable incidence angles and polarizations, as well as the use of cold sky for instrument calibration without the need for spacecraft maneuvers.

The beam from the mirror M2 is directed into the receiver unit (RU) box through a cutout in the rocker. The contents of the RU box are shown in Fig. 2. After entering the RU box, the beam meets a planar mirror M3 and an elliptical mirror M4 which reside on the rotational axis of the rocker structure. As the telescope is steered in the cross-track direction, the mirror M3 rotates together with the rocker and the telescope in such a way that the remaining beam path inside the RU box remains fixed. A free-standing wire grid (WG) splits the beam into two perpendicular polarizations. The transmitted polarization component is reflected from the elliptical mirror M5T to the smooth-walled spline-profiled feedhorn of the 1200-GHz double sideband (DSB) Schottky-mixer receiver [6]. The reflected polarization component is coupled via the elliptical

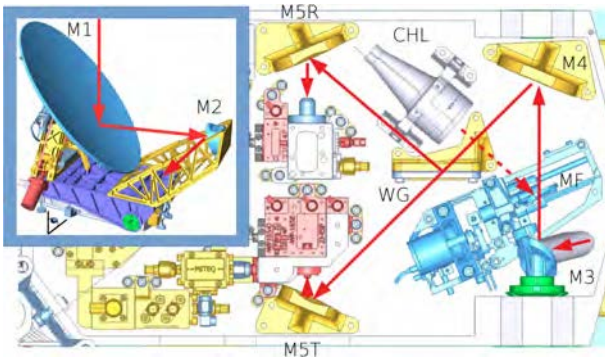

Fig. 2. Path of the optical beam in the receiver unit box (view from below, components attached to the RU box top cover).

mirror M5R to the corrugated feedhorn of the 600-GHz DSB Schottky-mixer receiver [7].

A conical blackbody calibration target (CHL) [8] acts as the hot temperature reference during the calibration. To allow the receivers to view the CHL, the beam between M3 and M4 is redirected by activating a planar flip mirror (MF).

A. Gaussian Beam Mode Analysis

Frequency independent operation has been one of the main design drivers which is achieved by imaging the aperture of the feedhorn onto the aperture of the primary mirror M1. In terms of Gaussian beam mode analysis, this means that the Gaussian beam phase shift between the feedhorn and M1 should be a multiple of π. Another constraint for the design is the edge taper requirement of at least 17 dB at M1 which together with the mirror diameter defines the maximum Gaussian beam radius.

The Gaussian beam best fitting to the simulated radiation pattern of the 600-GHz channel feedhorn has a beam radius of 0.851 mm and a radius of curvature of 8.35 mm at the feed aperture. The respective values for the 1200-GHz channel are 0.478-0.468 mm and 2.482-4.992 mm, depending on the frequency.

Table I presents the properties of the optical components and the results of the Gaussian beam mode analysis. Here, $f = (1/R_{in} + 1/R_{out})^{-1}$ is the effective focal length, d the distance to the previous component, R_{in} and R_{out} the radii of curvature of the conic mirror sections, w_i the incident beam radius at 530 GHz (row 1) and 1080 GHz (row 2), and θ_i the beam incidence angle. In case of M5R (M5T), d is the distance to the 600-GHz (1200-GHz) feedhorn aperture.

TABLE I
RESULTS OF GAUSSIAN BEAM MODE ANALYSIS

Comp.	f [mm]	d [mm]	R_{in} [mm]	R_{out} [mm]	w_i [mm]	$2\theta_i$ [deg]
M1	348.937	300.0	348.937	inf	98.848 98.872	90
M2	-64.0	241.0	209.179	-49.006	13.874 13.869	53.646
M3	inf	89.414	inf	inf	3.758 2.663	80.839
M4	59.714	72.186	105.854	136.998	9.081 8.397	45
WG	inf	92.814	inf	inf	3.108 3.108	90
M5R M5T	19.759 12.630	25.0 14.681	27.372 16.067	71.048 59.049	6.287 4.276	45 45

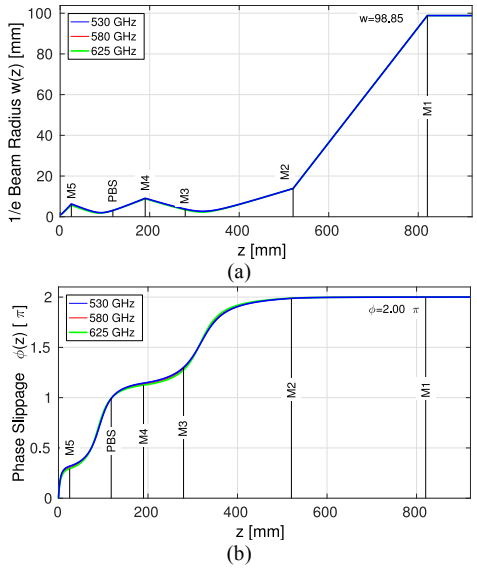

Fig. 3. Gaussian beam propagation along the 600-GHz beam path: a) radius, b) phase shift.

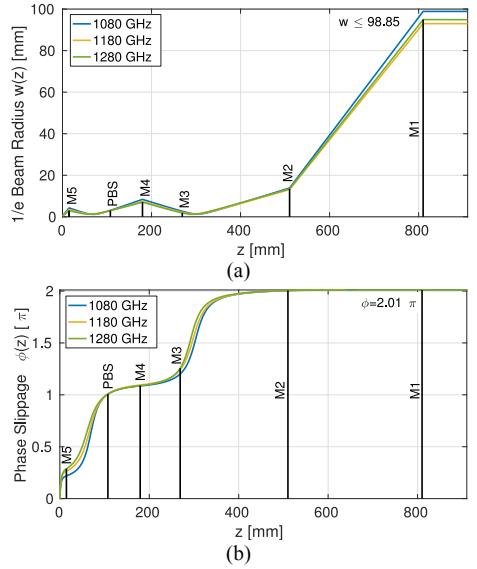

Fig. 4. Gaussian beam propagation along the 1200-GHz beam path: a) radius, b) phase shift.

Fig. 3 and Fig. 4 show the Gaussian beam radius and phase shift from the feedhorn aperture to the primary mirror M1 for the 600-GHz and 1200-GHz channels, respectively. The edge taper at M1 is approximately 18.7 dB which corresponds to a spillover loss of 1.4 %. The beam propagation in the 600-GHz channel is frequency independent, whereas the 1200-GHz channel exhibits some frequency dependency due to the frequency dependent input beam radius and radius of curvature.

B. Physical Optics Analysis

The Gaussian beam mode analysis does not include higher order modes or diffraction. The contribution of these effects has been accounted for in the PO analysis. Instead of the best-fit

Gaussian beams, the actual simulated far-field radiation patterns of the feedhorns have been used as an input.

First, the sizes of the optical components inside the RU box have been optimized for minimum spillover loss under mass and size constraints. The final projected radii are [R_{M3}, R_{M4}, R_{WG}, R_{M5R}, R_{M5T}] = [10, 19, 10, 16, 12] mm. Then the far-field radiation characteristics of the instrument have been simulated for the edge and center frequencies of each receiver channel. These are shown in Fig. 5 when the instrument points at the nadir, meaning that the telescope scan angles in the cross-track direction ϕ and in the along-track direction θ are zero. The key performance parameters obtained from the PO simulations are summarized in Table II.

The accumulated coupling efficiency at the mirror M1, η_{M1}, is > 98 %. Such a value is expected when one considers the M1 spillover loss of 1.4 % predicted by the Gaussian beam mode analysis. Losses due to the finite electrical conductivity of the optical surfaces are not included in η_{M1}. The maximum sidelobe and cross-polarization levels are below -20 dB. The latter is dominated by the 90° bend angle at M1 which is inherent to the instrument scanning concept. The absolute pointing errors of the 600-GHz and 1200-GHz beams in cross- and along-track directions are ≤ 0.16 arcmin. The requirement set by the science goals is less than 0.5 arcmin, but this includes the error contribution from the motors of the scanning mechanism and the alignment tolerance of optical components as well. The boresight direction of the 600-GHz and 1200-GHz beams on the sky agree to within 0.25 arcmin, the requirement being better than 1 arcmin.

The effect of telescope scanning in the cross-track direction is negligible, whereas scanning in the along-track direction causes the maximum cross-polarization level to increase: at the extremes of +72° and -72° the degradation is 1.2 dB and 2.5 dB, respectively. The pointing offsets, and consequently the coalignment of the beams, change as well, but the absolute errors remain approximately the same as for the nadir pointing.

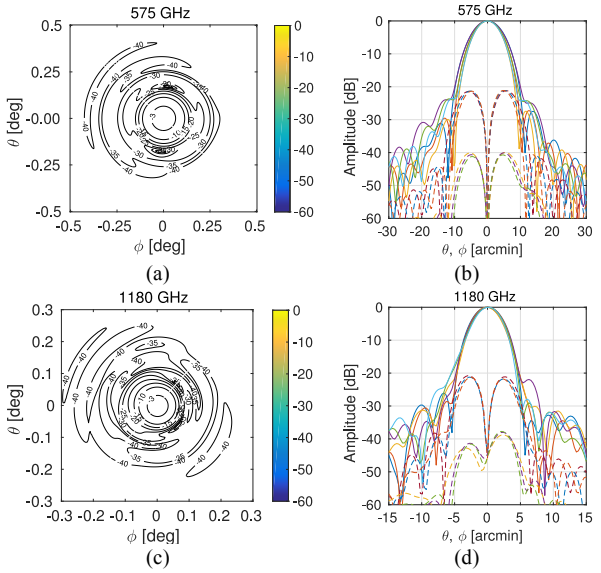

Fig. 5. Simulated SWI far-field radiation patterns: co-polar at a) 575 GHz and c) 1180 GHz; co-polar (solid) and cross-polar (dashed) at b) 530, 575, 620 GHz and d) 1080, 1180, 1280 GHz. The white lines in a) and c) indicate the polarization direction. The patterns in the planes $\theta = 0$ and $\phi = 0$ are included in b) and d).

TABLE II
RESULTS OF PHYSICAL OPTICS ANALYSIS

Freq. [GHz]	530	575	620	1080	1180	1280
Gain [dB]	62.63	63.41	64.07	68.94	69.21	69.56
η_{M1} [%]	98.14	98.34	98.61	98.02	98.03	98.07
FWHM [arcmin]	8.57	7.84	7.28	4.12	3.96	3.72
Max. cross-pol. level [dB]	-21.19	-21.11	-21.11	-20.80	-21.23	-21.30
Offset $\Delta\phi$ [arcmin]	-0.05	-0.04	-0.03	0.15	0.01	0.16
Offset $\Delta\theta$ [arcmin]	0.03	0.01	0.01	-0.11	-0.04	-0.10

CONCLUSIONS

The optical design and analysis of SWI on the JUICE spacecraft has been presented. The optical configuration is frequency independent in case of the 600-GHz receiver channel, whereas some frequency dependency is present in the 1200-GHz channel due to the frequency dependent properties of the beam launched by the 1200-GHz feedhorn. The pointing error due to the optics alone is the well below the specification of 0.5 arcmin. However, the contributions from the telescope scanning mechanism and the manufacturing and mounting tolerances of the optical components will be added to the error budget as well. Steering the telescope beam in the cross-track direction does not influence the optical performance, but along-track scanning increases the cross-polarization level up to 2.5 dB. Fortunately, the maximum degradation occurs at extreme scan angles that are only used for cold sky calibration that is not affected by the cross-polarization level.

ACKNOWLEDGEMENTS

The work at the University of Bern has been funded by the Swiss National Science Foundation under the Grant No. 200020-165744 and the ESA PRODEX program.

REFERENCES

[1] P. Hartogh *et al.*, "The submillimetre wave instrument on JUICE", in *Proc. EPSC 2013*, 2013, paper EPSC2013-710.

[2] M. A. Janssen *et al.*, "MWR: Microwave Radiometer for the Juno Mission to Jupiter," *Space Sci Rev,* vol. 213, no. 1-4, pp. 139-185, Nov. 2017.

[3] H. Kim, A. Murk, P. Hartogh, and SWI Team, "Optical Design Study for Submillimeter Wave Instrument for the Jupiter Mission," in *Proc. ISSTT 2015*, 2015, paper P-20.

[4] P. F. Goldsmith, *Quasioptical Systems*. Piscataway, NJ: IEEE Press, 1998.

[5] TICRA. GRASP 10.5.0. [Online]. Available: http://www.ticra.com/software/grasp

[6] A. Maestrini *et al.*, "1080-1280GHz Schottky Receiver for JUICE-SWI with 1600-2600K DSB Receiver Noise Temperature," in *Proc. ISSTT 2018*, 2018, paper M2.1.

[7] K. Jacob *et al.*, "Characterization of the 530 GHz to 625 GHz SWI Receiver Unit for the Jupiter Mission JUICE," in *Proc. 36th ESA Antenna Workshop,* 2015.

[8] K. Jacob, A. Schröder, M. Kotiranta, and A. Murk, "Design of the calibration target for SWI on JUICE," in *Proc. IRMMW-THz 2016*, 2016.